



SEISMIC RETROFITTING OF UNREINFORCED MASONRY WALLS BY CABLE SYSTEM

S. Chuang¹, Y. Zhuge², P.C. McBean³

SUMMARY

In the last two decades, several seismic retrofitting techniques for masonry structures have been developed and practiced, but rarely validated with experiments and numerical modelling. The purpose of this research is to develop a new and high strength seismic retrofitting technique for masonry structures. An innovative retrofitting technique with cable system is presented in this paper. In the paper, the experimental results of three unreinforced masonry walls retrofitted with cable system are presented. A nonlinear finite element model has also been developed for unreinforced masonry walls retrofitted by cable system to validate the experimental results. The results showed that both the strength and ductility of tested specimens were significantly enhanced with this new technique.

INTRODUCTION

Traditionally Australian civil engineers have not paid a great deal of attention to earthquake resistant design. However, the Newcastle earthquake in 1989 led to the creation of a new set of guidelines for earthquake resistance. This new code has resulted in the need to systematically retrofit structures that no longer comply with the new guidelines [1]. Masonry structures are one of the most common construction types in Australia. Although the history of past earthquakes has shown that masonry buildings have suffered the maximum damage and also accounted for the maximum loss of life, they continue to be popular. Most of the historic or existing buildings throughout Australia are unreinforced masonry, highlighting the need to improve their performance by retrofitting and strengthening to resist potential earthquake damages.

Un-reinforced masonry (URM) is one of the oldest and most widely used construction methods in the world. Inherent advantages, including; aesthetics, heat and sound insulation, fire resistance, economical considerations and sound understanding of its mechanical properties, contribute to its continuing appeal. In Australia the majority of URM buildings have been constructed with little or no seismic requirement. This has resulted in a large inventory of buildings that possess an inability to dissipate energy through inelastic deformation in an earthquake event. "Two types of failure are commonly observed in load

¹ S.W. Chuang, University of South Australia, Australia, shihwei.chuang@unisa.edu.au

² Y. Zhuge, Senior Lecture, University of South Australia, Australia, yan.zhuge@unisa.edu.au

³ P.C. McBean, Director, Wallbridge & Gilbert Consulting Engineers, pmcbean@wgeng.com

bearing URM walls subjected to seismic loads. These are in-plane failure characterized by a diagonal tensile crack pattern, and out-of-plane failure, where cracks are primarily along the mortar bed joints. [2] The aim of seismic retrofitting is to enhance the ultimate strength of the building by improving the structures ability to absorb inelastic deformation. This can be achieved by changing the structural system such that the energy is transferred along alternative load paths, or alternatively, increasing the ductility in the individual elements that make up the structural system. The application of cable system to URM is one method that attempts to improve a structures load carrying capacity and integrity during an earthquake event. With particular emphasis on in-plane failure, the project aims to investigate individual element strength improvements using cable system anchored to standard URM walls and the potential increases in ductility of indicative individual walls retrofitted accordingly, that might be included as part of a structural system.

Therefore, the best solution is to try to find a new material, which can provide higher strength and ductility, and the cost of material is cheap. Based on this objective, a new retrofitting method is being developed by using cable system. Cable systems have been used to upgrade URM buildings despite little experimental research. [3, 4, 5] Durgesh et al. (1992) tested a half-scale model of a URM wall strengthened by chevron steel braces [5]. It was concluded that the shear resistance of the rocking wall piers increased manifold due to steel vertical members. Braces added to the shear resistance of the wall while acting largely independent of the wall piers. The rocking controlled mode of the behavior of the wall piers did not alter due to steel braces and verticals.

Cable consists of a number of wires or strands and has high tensile strength, lightness and high corrosion resistance. These materials can absorb tensile stress and increase overall element stiffness, ductility and bearing capacity. Using cable system for seismic retrofitting applications has other advantages such as architectural versatility, low cost and fast construction, durability, and no loss of valuable space. Furthermore, it does not add a significant mass to the existing building and can remain unchanging dynamic properties for structures. Therefore, Cable would be seen to be particularly suitable for seismic retrofitting materials.

EXPERIMENTAL PROGRAM

Three full-scale clay brick masonry walls retrofitted with cable system and one full-scale clay brick unreinforced masonry wall have been tested under combined compression and racking cyclic loads.

Test specimen

To simulate practical situations, solid clay bricks (Medium Sandstock, Size of brick: 230x110x76mm) which are commonly used as load bearing walls in Australia were chosen from commercially available clay bricks to build the test wall panels. The mortar used had a mix design of 1:1:6 (cement: lime: sand, by volume) ratio and a thickness of 10mm. To maintain the consistency, all the wall panels were built by the same bricklayer and were cured in air for 28 days, before testing. The test wall panels were built on reinforced concrete beams which were bolted on to the reaction floor. The beams acted as a foundation for the walls.

The type of cable used for this experiment was Ronstan typical grade 316 stainless steel wire rope (19 single strands, Diameter 10mm, and breaking load 71 KN) and ending for cable was sea-fast threaded swage terminals (RF1513M1010). The anchorage for the connection plate to the foundation beam was Ramset Chemset Anchor. (M 16x190mm, design tensile and shear load 8.5KN per anchor and Chemset 800 series). The cable was fixed on one side of the wall only.

Wall configuration

Wall with aspect ratios of less than 1.0 have flexural strength higher than their shear strength [6, 7, 8]. These walls should fail in shear in a non-ductile manner. The proposed retrofitting systems aim to improve the performance of walls by increasing shear strength above their flexural strength and by increasing ductility and energy dissipation capability. All specimens were chosen with an **aspect ratio of 1.0** to ensure that most of the unretrofitted walls would exhibit shear-induced damage. Therefore, the in-plane failure would be dominated. The dimension of the wall is 940mm long x 940mm high x 110 wide (11 courses high and 4 bricks in each course). The wall was constructed on top of a concrete foundation beam to simulate a house footing.

The detailed design for the cable system

Retrofit was accomplished by adding two 10mm diameter cables (wire ropes) on only one side of the wall face, as shown in Figure 1. Cables should be added on both sides of the wall to prevent an eccentric stiffness and strength distribution that may cause twisting of the retrofitted walls, enhance redundancy of the retrofitted walls, and provide simultaneous retrofit against out-of-plane failures of walls (although this was not tested in this investigation). The details of the cable system design were shown in Fig 1. The cable diameter was chosen to ensure that the wall will fail earlier than the cable. The anchor was design for transferring the load from cable to foundation without failure before the cable is broken. The cable was carried about 25KN when the wall was loaded about 50KN.

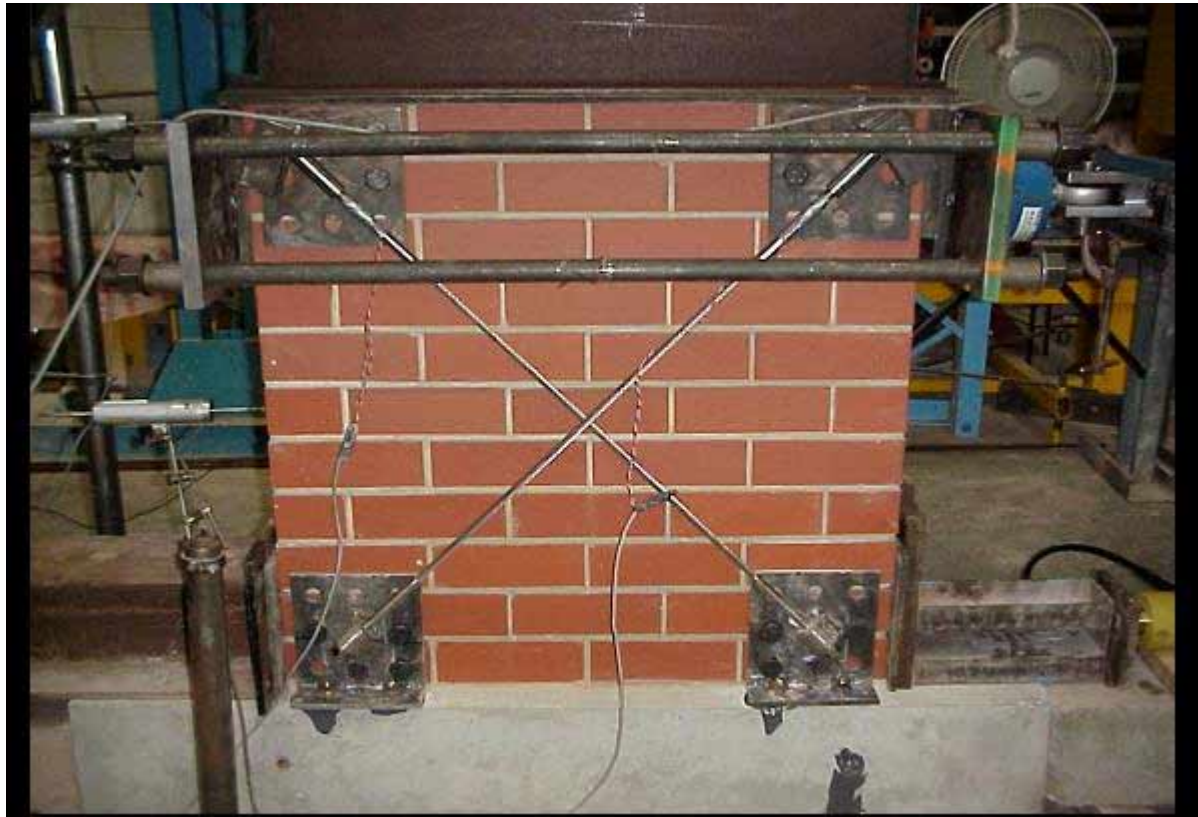


Figure 1. Wall retrofitted using cable systems

Testing setup

The test setup is shown in Figure 2. One hydraulic jack was used to apply lateral loads to the specimen and another one used to apply a vertical load. The jacks were supported by a steel reaction frame. The vertical load was applied uniformly to the top of the wall through a stiff spreader beam. The walls were braced by using two lateral steel beams to prevent the out-of-plane deflection.



Figure 2. Test setup

Loading history

Each specimen was subjected to horizontal displacement reversals while also subjected to a constant axial compression. In this testing program, axial loads were applied to all specimens in addition to the lateral loads, to create a more realistic loading condition, and because this research includes masonry walls whose ultimate behaviour is considerably affected by the presence of gravity loads. For example, the rocking capacity of URM walls depends directly on the magnitude of the applied axial load. If bearing loads are not applied on such a masonry wall, its lateral capacity is theoretically zero (if the self weight of the wall is neglected). Identical axial loads were applied to all specimens of this research. This simulated identical tributary floor areas, and made it convenient to compare the results between specimens. A realistic axial load of 0.2 MPa was applied to the wall to simulate an applied roof and second story onto

the wall. To simulate earthquake loading, a series of horizontal displacement cycles of increasing amplitude were used on all the walls. The wall was cycled twice at each of the incrementally increasing inelastic displacement amplitude until failure.

EXPERIMENTAL RESULTS

The three walls tested had the same height-to-thickness ratio, and were retrofitted using the same cable system. The load-deflection envelopes for three walls are compared with an un-retrofitted wall in Fig 3. It can be seen from the envelope, the dramatic increase of the ultimate strength for walls retrofitted with cable is evident. The improvement of the ultimate lateral load resistance of the retrofitted walls with cable system is about 2 times the capacity of unretrofitted wall. From the Fig. 3, it shows that URM wall is strongly nonlinear at low level of load due to the low tensile strength of bed and head joints. It also shows that URM wall decreased both strength and stiffness as the damage due to cracking increases. As it can be seen from the figure, the URM walls retrofitted by the cable system slowed down the cracking propagation and increased both strength and stiffness.

All wall specimens retrofitted using the proposed cable system concept exhibited superior behavior when compared with the unretrofitted wall specimens. The hysteretic relationship of all wall specimens is shown in Figures 4, 5 and 6, respectively, indicates that the retrofitted URM walls exhibit good strength, ductility, stiffness, and dissipation of energy compared with the unretrofitted wall. From the hysteretic relationship of URM wall, it shows that the wall behaved in a combination of rocking and sliding as evidenced by the unsymmetric hysteresis loops. It also shows that the flexural response is occurred because very large displacements were obtained without significant loss in strength. From the hysteretic relationship of retrofitted walls, it shows that the walls behaved in shear cracking response as evidenced by the significant loss in strength at post-peak response of hysteresis loops.

The unretrofitted wall behaved in a combination of the sliding developed in one direction and the rigid-body rocking (with some small amount of sliding) developed in the other direction. As you can see from the hysteretic relationship of URM wall in Fig.4, the hysteretic energy dissipated in a rocking mode response is generally smaller and the hysteretic energy dissipated in a sliding mode response is higher. As you can see from the hysteretic relationship of retrofitted walls in Fig.4, 5, and 6, the hysteretic energy dissipations are much higher than URM wall because the effectiveness of cable system in distributing the cracks over the entire wall increased the whole wall energy dissipation.

Variation in stiffness with lateral drift is plotted in Fig. 7 for all the walls. The stiffness at every drift level was calculated using the two-peak value of each cycle. Only the first cycle of each drift was considered. The stiffness of each cycle was computed using the peak-to-peak method. The curves indicated the sensitivity of the stiffness of each specimen with respect to the top horizontal displacement. As can be seen from the figure presented, stiffness of retrofitted walls significantly improved compared to the unretrofitted wall.

The force carried by cable and force carried by the whole retrofitted wall is shown in Fig 8, 9 and 10, respectively, indicate that the cable carried about the 50% of force acted on the whole wall. In these figures, they also shows that the cables start to carry the force at the very beginning stage. That means the URM wall retrofitted by cable system becomes a whole new structure to carry the force together.

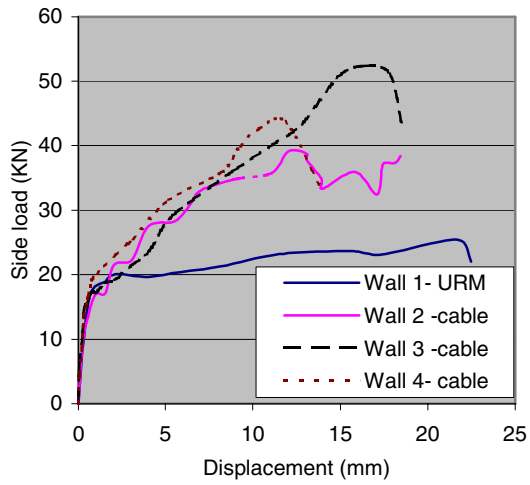


Figure 3. The load-deflection envelope

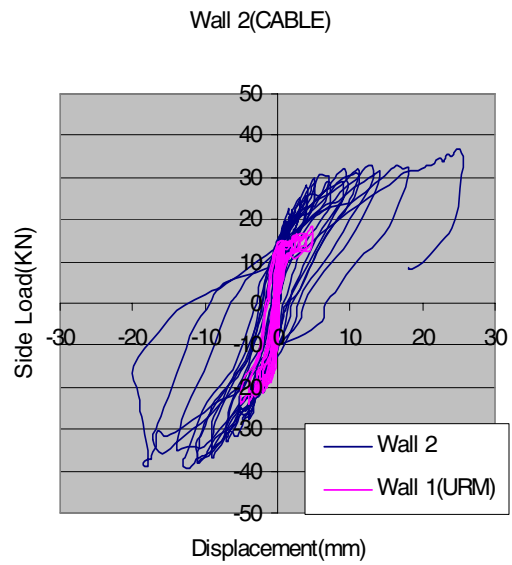


Figure 4. Hysteretic behaviour of Wall-2

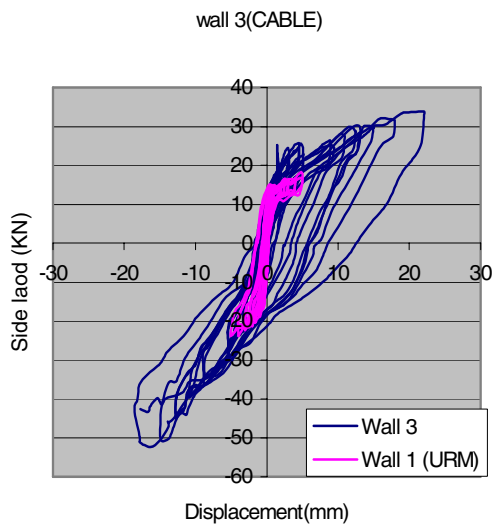


Figure 5. Hysteretic behaviour of Wall-3

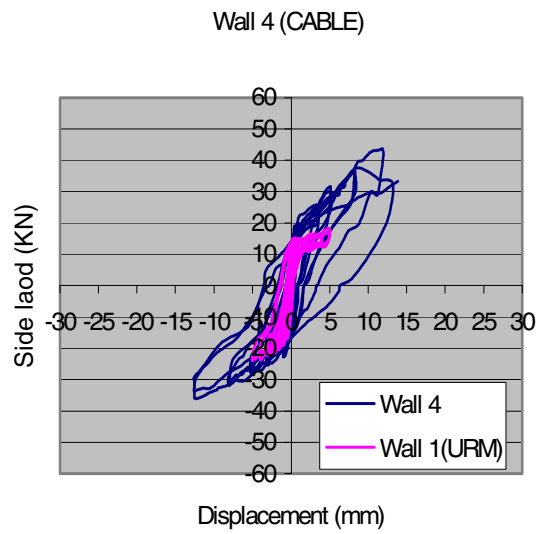


Figure 6. Hysteretic behaviour of Wall-4

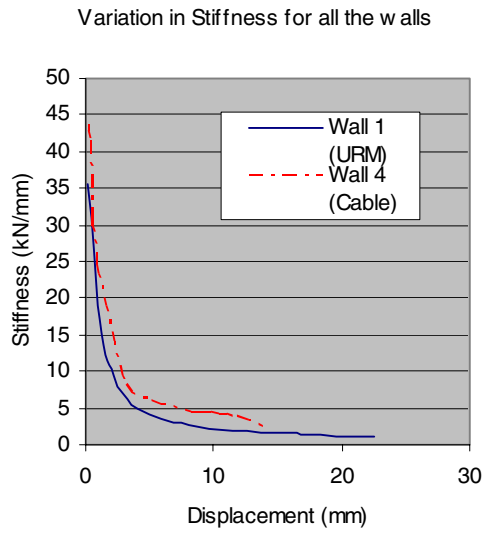


Figure 7. Variation in Stiffness for all walls

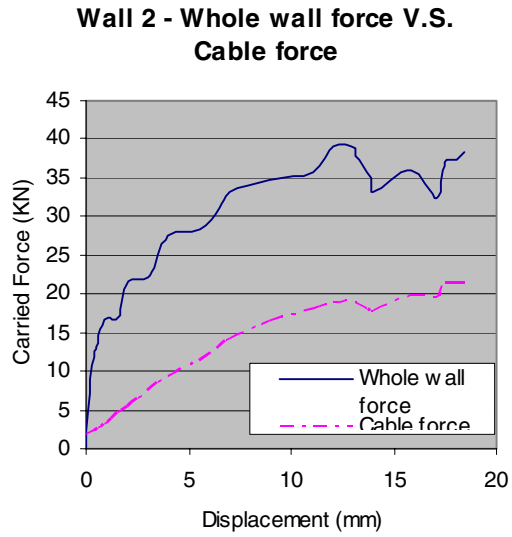


Figure 8. The load-deflection envelope of Wall2 (Retrofitted with cable)

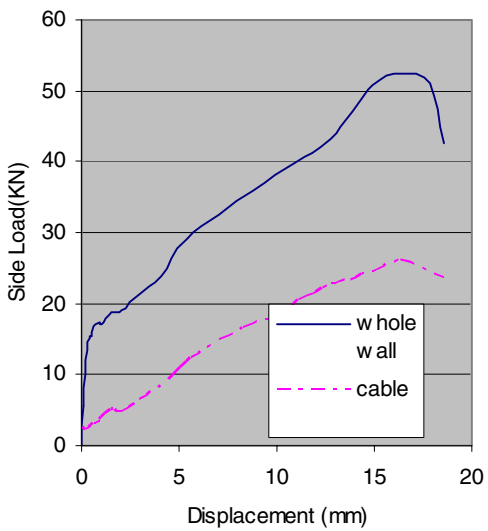


Figure 9. The load-deflection envelope of wall 3

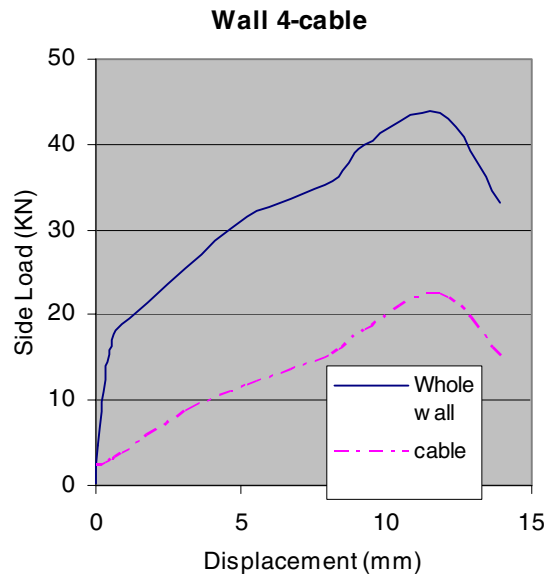


Figure 10. The load-deflection envelope of Wall 4

FINITE ELEMENT MODELLING

Modeling techniques for unreinforced masonry wall

Masonry is a composite material that consists of units and mortar joints. In general, the approach towards its numerical representation can focus on the micro-modelling of masonry as a component, such as unit (brick, block, etc.) and mortar, or the macro-modelling of masonry as a composite [9]. Depending on the level of accuracy and the simplicity desired, it is possible to use the following modeling strategies, see Figure 11.

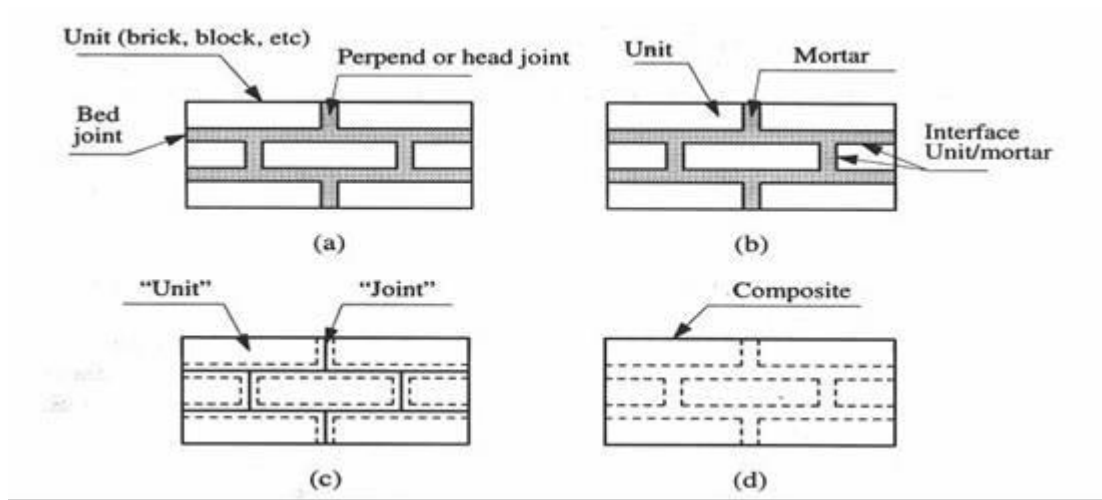


Figure 11 Modelling strategies for masonry structures: (a) masonry sample;(b) detail micro-modelling;(c) simplified micro-modelling;(d) macro-modelling [10]

- Detailed micro-modelling – units and mortar in the joints are represented by continuum elements whereas the unit-mortar interface is represented by discontinuous elements;
- Simplified micro-modelling - expanded units are represented by continuum elements whereas the behavior of the mortar joints and unit-mortar interface is lumped in discontinuous elements;
- Macro-modelling – unit, mortar and unit-mortar interface are smeared out in the continuum.

The macro-modelling is more practice oriented due to the reduced time and memory requirements as well as a user-friendly mesh generation. This type of modeling is most valuable when a compromise between accuracy and efficiency is needed. In this paper, the macro-modelling is adopted to model the unreinforced wall retrofitted by cable system. Masonry is a composite material. It consists of bricks and mortar joints. The macro-modelling does not make a distinction between individual units and joints but treats masonry as a homogeneous anisotropic continuum. Masonry can be assumed to be a homogeneous material if a relation between average stresses and strains in the composite material is established. For the numerical analysis, bilinear plane stress continuum elements with full gauss integration are utilized.

Selection of element type

Numerical modeling was carried out using the finite element code ABAQUS. For macro-modelling, the four-node bilinear two-Dimensional plane stress element, CPS4R, was used to model the masonry. A more sophisticated element, such as the eight-node isoparametric element, was not used because it has been shown from previous research [11,12] that the use of higher order elements was not warranted for the analysis of brick masonry (where nonlinearity is mainly due to progressive cracking and not non-linear

material characteristics), provided a relatively fine element mesh was adopted. The four-node bilinear two-Dimensional plane stress element, CPS4R, was also used to model the steel plates that used to connect between the cable and masonry wall. The two-Dimensional truss element, T2D2, was used to model the cable. The 2-node straight truss element uses linear interpolation for position and displacement and has a constant stress. The truss element is long, slender structural members that can transmit only axial force. No Compressive option was used to make sure the cable only takes tension. The element has two degrees of freedom at each node and translations in the nodal x and y directions. The connector element, connection type BEAM, was used to model Connection between the steel plate and masonry wall. This connector element, BEAM, provides a rigid beam connection between two nodes.

Constitutive law of Masonry

A constitutive model is a mathematical description of material behaviour. There are two major aspects to develop an accurate analytical model. One is to understand the material behaviour of masonry which is the constitutive relations of the material, the other is the failure criteria of the material because the major nonlinear effect of URM under in-plane lateral load is due to progressive cracking. [13]

Development of a model for the behavior of masonry is a challenging task. Masonry is a quasi-brittle material and has different behavior in compression and tension. Figure 12 shows a typical stress-strain curve for clay-brick masonry.

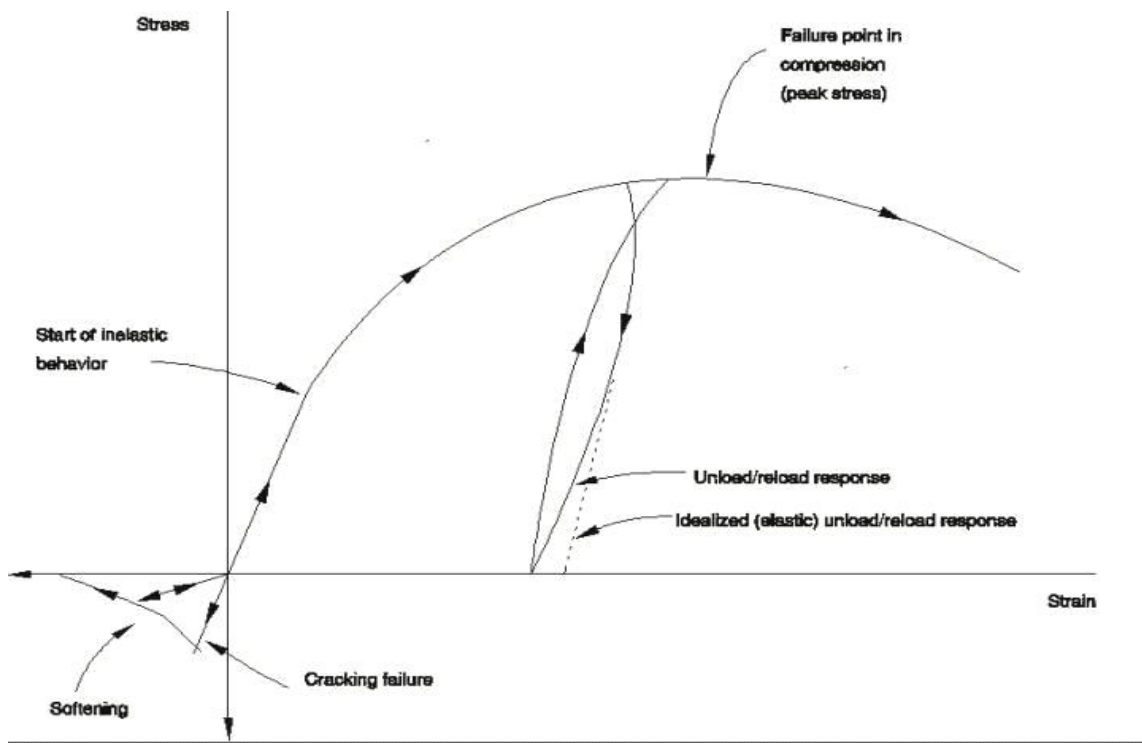


Figure 12 A typical stress-strain curve for clay-brick masonry

Most masonry walls subjected to in-plane loads are in a state of biaxial stress, therefore it is necessary to consider a biaxial stress-strain model for masonry [13]. The proposed model is capable of predicting failure of masonry materials. Both cracking and crushing failure modes are accounted for. The two input

strength parameters-i.e., ultimate uniaxial tensile and compressive strengths are needed to define a failure surface for the masonry. Consequently, a criterion for failure of the masonry due to a multiaxial stress state can be calculated. A two-dimensional failure surface for masonry is shown in Figure 13. For masonry, cracking occurs when the principal tensile stress in any direction lies outside the failure surface. After cracking, the elastic modulus of the masonry element is set to zero in the direction parallel to the principal tensile stress direction. Crushing occurs when all principal stresses are compressive and lies outside the failure surface; subsequently, the elastic modulus is set to zero in all directions [14], and the element effectively disappears.

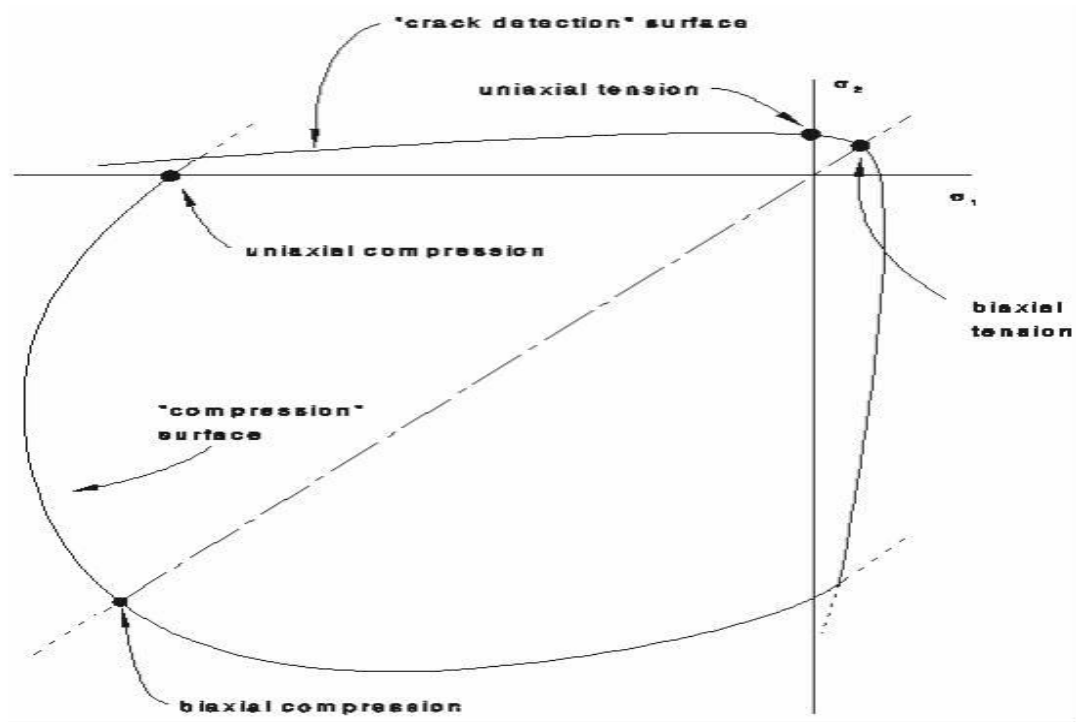


Figure 13 A two-dimensional failure surface for masonry

Finite element discretization

As an initial step, a finite element analysis requires meshing of the model. In other words, the model is divided into a number of small elements, and after loading, stress and strain are calculated at integration points of these small elements [15]. An important step in finite element modelling is the selection of the mesh density. A convergence of results is obtained when an adequate number of elements are used in a model. This is practically achieved when an increase in the mesh density has a negligible effect on the results [16]. Figure 14 shows meshing for the retrofitted wall model.

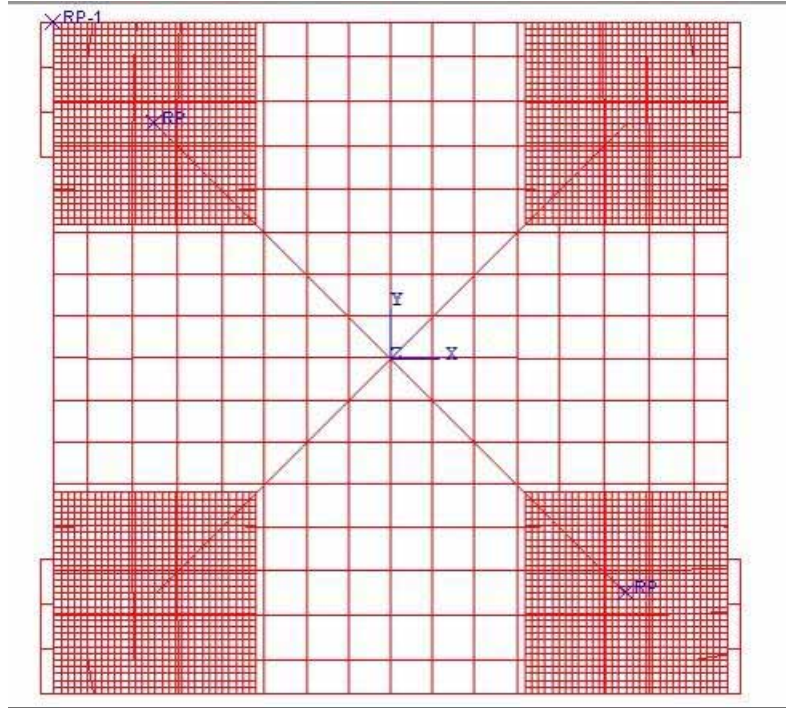


Figure 14 The mesh for the retrofitted wall model

VALIDATION OF THE NUMERICAL MODEL RESULTS

This paper compares the results from ABAQUS finite element analyses with experimental results of four masonry walls. The following comparisons are made: load-deflection plots; first cracking loads; loads at failure; and forces carried by cable. The data from the finite element analyses were collected at the same locations as the experimental tests.

Load-deflection plots

Force-displacement relationships from finite element models described in this paper have been compared with experimentally obtained envelopes. These results are presented in Figs 15, 16 and 17 for URM wall and retrofitted walls, respectively. The numerical models provide good correlations with test data and can be considered as effective analytical tools.

Figure 15 shows that the load-deflection plot from the finite element analysis agrees well with the experimental data for the URM wall. The load-deflection plot from the finite element analysis is slightly stiffer than that from the experimental results. This is possibly due to the relative homogeneity of the finite element models when compared to the relative non-homogeneity of the actual walls that contain two different materials and neglect the weaker mortar plane effect. The first cracking load of the finite element analysis is 15.2 KN, which is higher than the load of 14.7 KN from the experiments by only 4%. Lastly, the ultimate load predicted by the finite element model is 24.4 KN which is higher than the ultimate load of 22.49 KN from the experimental data by only 8 %.

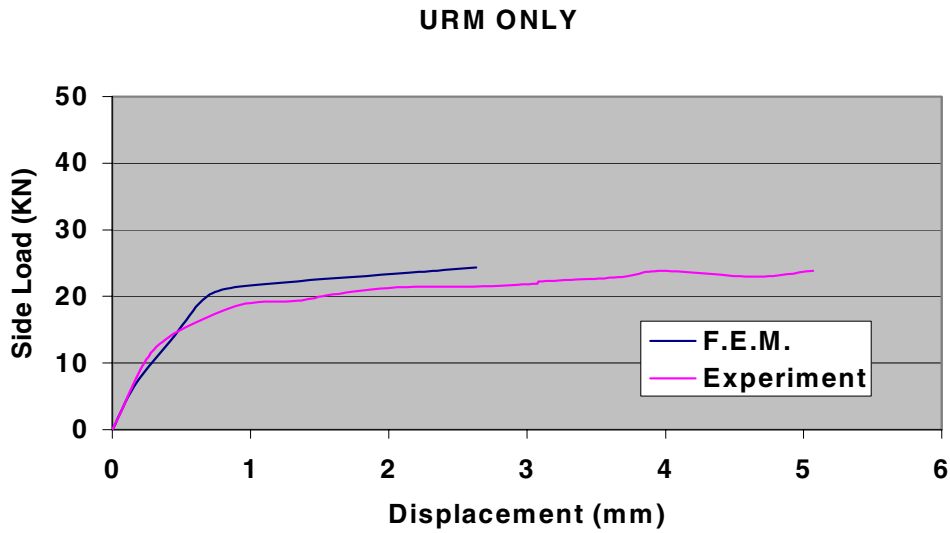


Figure 15 Load-deflection comparison for URM wall

Figure 16 shows that the load-deflection plot from the finite element analysis agrees well with the experimental data for the retrofitted wall with cable. The load-deflection plot from the finite element analysis is stiffer than that from the experimental results. This is possibly due to the fatigue of the material. The results from the finite element model subject to monotonic loading, but the results from experiment subject to cyclic loading. The first cracking load for the finite element analysis is 17.5 KN, which is higher than the load of 15.2 KN from the experimental results by 15%. Lastly, the ultimate load predicted by the finite element model is 49.15KN which is higher than the ultimate load of 46.4 KN from the experimental data by 6 %.

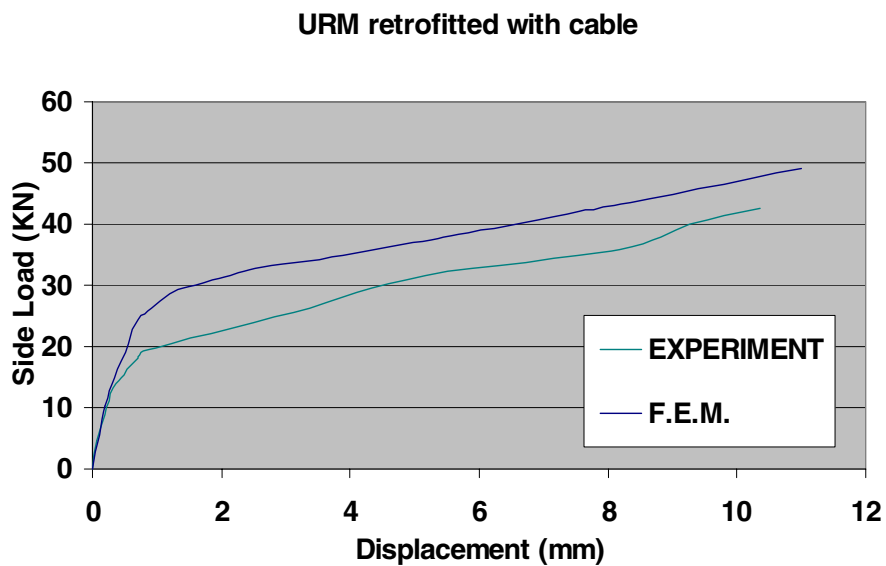


Figure16 Load-deflection plot for URM wall

Figure 17 shows that the load-deflection curve for the URM wall before and after retrofitting with cable from the finite element analysis. The load-deflection curve for retrofitted wall is much stiffer than the unreinforced wall. In this figure, it also shows that the retrofitted wall significantly increases the strength and ductility of the unreinforced masonry wall. These results are similar to the experimental results. The improvement of the ultimate lateral load resistance of the retrofitted walls with cables is 2 times the capacity of unreinforced wall. The improvement of the ductility of the retrofitted walls with cables is about 6 times the capacity of unreinforced wall.

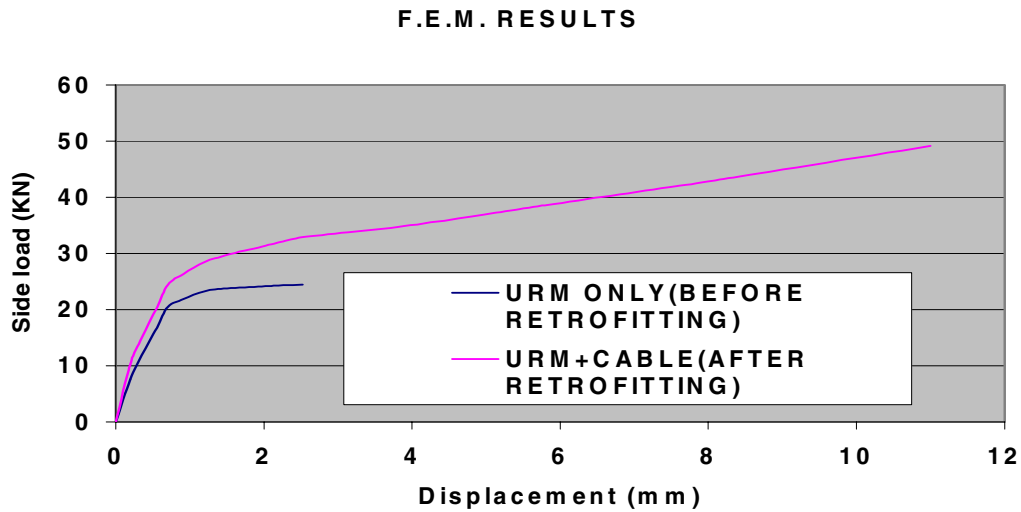


Figure 17 Load-deflection plot for before retrofitting and after retrofitting

First cracking loads

The first cracking load from the finite element analysis is the load step where the first signs of cracking occur for masonry in the model. Loads at first cracking from the finite element model and the experimental results are compared in Table 1.

Table 1 Comparisons between experimental and ABAQUS first cracking loads

Retrofitting Methods	Experiment	F.E.M.	% Difference
URM	14.7KN	15.2KN	4%
CABLE	15.2KN	17.5KN	15%

The first cracking loads from the finite element analyses and the experimental data are within 15% for URM wall and retrofitted walls. In all cases, the first cracking load from ABAQUS is higher than that from the experimental data. This is possibly due to the relative homogeneity of the finite element models when compared to the relative heterogeneity of the actual walls that contain a number of microcracks.

Loads at failure

Table 2 compares the ultimate loads for the URM wall and retrofitted walls. In general, the ultimate loads predicted by the finite element model are higher than the experimental results. Several reasons could be attributed to this. The material properties assumed in this study may be imperfect. The stress-strain curve

for the cable used for the finite element models was not obtained directly from material testing. The actual cable may have a different stress-strain curve when compared to the idealized one, as shown in Figure 8. Therefore, this may help to produce the higher ultimate load in the finite element results.

Table 2 Comparisons between experimental and ABAQUS loads at failure

Retrofitting Methods	Experiment	F.E.M.	% Difference
URM	22.49KN	24.4KN	8%
CABLE	46.4KN	49.15KN	6%

Forces carried by cable

For the actual retrofitted walls, there was no evidence that the cable failed before overall failure of the walls. This is confirmed by the finite element analyses. In the figure 18, the forces carried by the cable from ABAQUS are compared to the results obtained from the experimental tests. It can be seen from the figure, at the ultimate load of the wall, the force carried by the cable is around 25 KN which is far less than the load capacity of the cable.

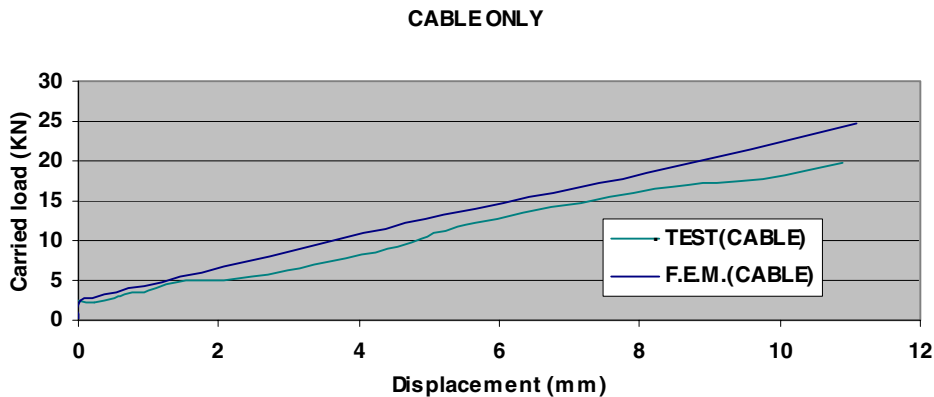


Figure 18 Comparison between experimental and ABAQUS for carried force by cable

CONCLUSIONS

Experiments conducted in this study show that cable system retrofitted to low-rise masonry walls are effective in significantly increasing their in-plane strength, ductility, and energy dissipation capacity. The improvement of the ultimate lateral load resistance of the retrofitted walls with two cables strengthening is 2 times the capacity of unreinforced wall. Note that, although no out-of-plane tests were conducted within the scope of this research, the authors believe it is preferable to use the proposed strip system on both sides of the wall, to provide greater out-of-plane strength and minimize out-of-plane displacements.

Non-linear finite element models were developed to predict strength and ductility of URM wall and URM walls retrofitted with cable system. The experimental results obtained from URM walls retrofitted with cable system are compared with those obtained from analytical solutions. The analytical results were obtained using finite element program ABAQUS. The proposed finite element model has the ability to track the behaviour of URM wall and URM wall retrofitted with cable from the first cracking almost to final failure. The results obtained from these models also show good agreement with the experimental

results. Seismic retrofitting of unreinforced masonry walls with cable system proved to be an effective and reliable strengthening alternative.

ACKNOWLEDGEMENTS

Financial support for the present study was provided under Department for Administrative and Information Services at South Australia Government. This support is gratefully acknowledged. The writers would also like to thank university technical officers Gerry Lewis, Raymond Yerbury, Colin Sharpe for their contribution to this project.

REFERENCES

1. DAIS, "Strengthening existing buildings for earthquakes." *Building Management, Department for Administrative and Information Services*, South Australia, 2001.
2. Ehsani MR, Saadatmanesh H and Velazquez-Dimasi JI. Behaviour of retrofitted URM walls under simulated earthquake loading. *Journal of Comp for Constr*, ASCE, 1999; 3(3): 134-142.
3. Pincherira, J.A. and Jirsa, J.O. "Post-tensioned bracing for seismic retrofit of RC frames." *Proceedings of the 10th World Conference on Earthquake Engineering*, 1992, Vol. 6: 5199-5204.
4. Sittipunt, C., Wood, S.L., Lukkunaprasit, P., and Pattararattanukul, P. "Cyclic behaviour of reinforced concrete structural walls with diagonal web reinforcement." *ACI Structural Journal*, 2001, July-August, 555-563.
5. Durgesh C. R., Subhash C. G., and William T.H. "Seismic strengthening of URM buildings with steel bracing." *Earthquake Spectra*, 1992, 12(4): 697-705.
6. Taghdi, M. "Seismic retrofit of low-rise masonry and concrete walls by steel strips." *Thesis presented Dept. of Civ. Engrg.*, Univ. of Ottawa, in partial fulfillment of the requirements for the degree of Doctor of Philosophy, Ottawa, 1998.
7. Taghdi, M., Bruneau, M., and Saatcioglu, M. "Seismic retrofitting of low-rise masonry and concrete walls using steel strips." *J. Struct. Engrg.*, 2000, ASCE, 126(9), 1017-1025.
8. Taghdi, M., Bruneau, M., and Saatcioglu, M. "Analysis and design of low-rise masonry and concrete walls retrofitted using steel strips." *J. Struct. Engrg.*, 2000, ASCE, 126(9), 1026-1032.
9. Rots, J.G., Numerical simulation of cracking in structural masonry, Heron, 1991, 36(2), p.49-63.
10. Lourenco, P. B. Computational strategies for masonry structure, Delft University Press, The Netherlands, 1996.
11. Bazant, Z. P. and Cedolin, L., Fracture Mechanics of Reinforced Concrete, Journal of the Engineering Mechanics Division, 1980, Vol. 106, No. EM6, pp. 1287-1306.
12. Ail, S., 1987, Concentrated Loads on Solid Masonry, PhD Thesis, University of Newcastle.
13. Zhuge, Y., Nonlinear Dynamic Response of Unreinforced Masonry under In-Plane Lateral Loads, PhD Thesis, Queensland University of Technology, 1996,
14. HKS, ABAQUS/standard user's manual, version 5.5, Hibbitt, Karlson and Sorensen, Pawtucket, R.I, 2002.
15. Bathe, K.J., Finite Element Procedures, Prentice-Hall, INC., Upper Saddle River, New Jersey, 1996,
16. Adams, V. and Askenazi, A., "Building Better Products with Finite Element Analysis." On Word Press, santa Fe, New Mexico, 1998.